

Theoretical Study of the Hydrogen-Abstraction Reactions for $\text{CH}_3\text{CX}_3 + \text{Cl} \rightarrow \text{CH}_2\text{CX}_3 + \text{HCl}$ ($\text{X} = \text{Cl}$ and F)

Jing-Fa Xiao, Ze-Sheng Li,* Jing-Yao Liu, Li Sheng, and Chia-Chung Sun

Institute of Theoretical Chemistry, State Key Laboratory of Theoretical and Computational Chemistry, Jilin University, Changchun 130023, P. R. China

Received: August 28, 2002; In Final Form: November 11, 2002

The dynamical properties for the two hydrogen-abstraction reactions of 1,1,1-trichloroethane (CH_3CCl_3) and 1,1,1-trifluoroethane (CH_3CF_3) with chlorine atoms over the temperature range 200–1200 K are investigated theoretically. The minimum energy paths (MEPs) of both reactions are calculated at the BH&H-LYP/6-311+G(d,p) level, and the energies along the MEPs are further refined at the CCSD(T)/6-311+G(2df,2p) (single-point) level. For both reactions, the theoretical rate constants are in good agreement with available experimental results. Compared with the one previous theoretical investigation at the HF/6-31G(d) level followed by BAC-MP4 single-point energy calculations, our calculated rate constants are closer to the experimental values. The theoretical results show that for the title reactions the variational effect is small over the whole considered temperature range and the small-curvature tunneling effect is only important in the lower temperature range.

Introduction

The hydrogen-abstraction reactions of halogen-substituted hydrocarbons with chlorine atoms play an important role in the processes of industrial chlorination and atmospheric chemistry in the lower temperature range.¹ High-quality kinetic data for these reactions, especially at elevated temperatures, are crucial for modeling these processes accurately. Hydrochlorofluorocarbons (HCFCs) and hydrofluorocarbons (HFCs) are two classes of potential chlorofluorocarbon (CFC) substitutes. To evaluate the atmospheric effect of hydrochlorofluorocarbons and hydrofluorocarbons as substitutes for fully halogenated species in industrial applications, many kinetic studies have been made to determine the rate and the mechanisms of these reactions. In this paper, we focus our attention on the hydrogen-abstraction reactions for 1,1,1-trichloroethane (CH_3CCl_3) and 1,1,1-trifluoroethane (CH_3CF_3) by chlorine atom attack, that is, $\text{CH}_3\text{CCl}_3 + \text{Cl} \rightarrow \text{CH}_2\text{CCl}_3 + \text{HCl}$ and $\text{CH}_3\text{CF}_3 + \text{Cl} \rightarrow \text{CH}_2\text{CF}_3 + \text{HCl}$. There have been some experimental studies available in the literature concerning rate constants for the reactions $\text{CH}_3\text{CCl}_3 + \text{Cl}^{2-6}$ and $\text{CH}_3\text{CF}_3 + \text{Cl}^{7,8}$. For both reactions, the agreement among most of the experimental data is good.

In contrast to the large number of experimental studies, theoretical investigations on the kinetic parameters of the title reactions are rather limited. In 1992, Senkan and Quam⁹ calculated the rate constants of both reactions by using Evans–Polanyi and structure–activity relationships methods. In 1996, Rayez and co-workers⁶ obtained the 298 K rate constant as $6.8 \times 10^{-15} \text{ cm}^3 \text{ molecule}^{-1} \text{ s}^{-1}$ for reaction $\text{CH}_3\text{CCl}_3 + \text{Cl}$ and $5.7 \times 10^{-16} \text{ cm}^3 \text{ molecule}^{-1} \text{ s}^{-1}$ for reaction $\text{CH}_3\text{CF}_3 + \text{Cl}$ at the HF/6-31G(d) level followed by BAC-MP4 single-point energy calculations. For the reaction $\text{CH}_3\text{CCl}_3 + \text{Cl}$, the rate constant of Rayez and co-workers is in good agreement with the experimental value,⁶ $7.1 \times 10^{-15} \text{ cm}^3 \text{ molecule}^{-1} \text{ s}^{-1}$. But, for the reaction $\text{CH}_3\text{CF}_3 + \text{Cl}$, their calculation overestimated

the experimental values,⁷ $2.5 \times 10^{-17} \text{ cm}^3 \text{ molecule}^{-1} \text{ s}^{-1}$, over 20 times. In addition, they did not report the rate constants at other temperatures. To take into account the discrepancies between experiment and theoretical investigation, one aim of this paper is to perform a direct ab initio dynamics study at a relatively higher level on the rate constants of the hydrogen-abstraction reaction by Cl over the temperature range 200–1200 K to obtain more reliable results.

Calculation Methods

In our study, standard ab initio and DFT calculations are carried out with the Gaussian 98 program.¹⁰ Equilibrium geometries and frequencies of the stationary points (reactants, products, and transition states) are calculated by using Becke's half-and-half (BH&H) nonlocal exchange and the Lee–Yang–Parr (LYP) nonlocal correlation functionals with the 6-311G+(d,p) basis set. At the same level, the minimum energy path (MEP) is obtained by using intrinsic reaction coordinate theory (IRC) with a gradient step size of 0.05 (amu)^{1/2} bohr. Furthermore, at 16 selected points (8 points in the reactant channel, 8 points in the product channel) along the MEP, the force constant matrices, as well as the harmonic vibrational frequencies (wavenumbers), are obtained. Furthermore, the energies of MEP are further refined at the CCSD(T)/6-311+G-(2df,2p) level. To obtain the rate constants theoretically for the temperature range 200–1200 K, the POLYRATE, version 8.4.1, program¹¹ is employed with the aid of the conventional transition-state theory (TST) and the improved canonical variational transition-state theory (ICVT)¹² incorporating the small-curvature tunneling correction (SCT) method proposed by Truhlar and co-workers.^{13,14} The rate constants are calculated at 200–1200 K temperatures using mass-scaled Cartesian coordinate. The Euler single-step integrator with a step size of 0.0001 (amu)^{1/2} bohr is used to follow the MEP, and the generalized normal-mode analysis is performed in every 0.01 (amu)^{1/2} bohr. The curvature components are calculated using

* To whom correspondence should be addressed.

TABLE 1: Calculated and Experimental Geometrical Parameters (Distance in Å and Angle in deg) of Stable Structures

species	geom params	calcd ^a	expt ^b
CH ₃ CCl ₃ (C _{3v})	R _{CC}	1.508	1.460
	R _{CCl}	1.783	1.771
	R _{CH}	1.083	1.090
	∠HCC	109.5	108.9
	∠ClCC	110.0	109.6
CH ₂ CCl ₃ (C _s)	R _{CC}	1.465	
	R _{CCl'}	1.809	
	R _{CCl}	1.781	
	R _{CH}	1.073	
	∠Cl'CC	109.5	
	∠ClCC	110.6	
	∠HCC	118.8	
CH ₃ CF ₃ (C _{3v})	∠HCH	121.0	
	R _{CC}	1.493	1.494
	R _{CF}	1.334	1.340
	R _{CH}	1.083	1.081
	∠HCC	109.2	112.0
CH ₂ CF ₃ (C _s)	∠FCC	111.9	119.2
	R _{CC}	1.472	
	R _{CF'}	1.341	
	R _{CF}	1.332	
	R _{CH}	1.073	
	∠F'CC	112.1	
	∠FCC	111.8	
HCl	∠HCC	118.8	
	∠HCH	121.8	
	R _{HCl}	1.275	1.275

^a Calculated at the BH&H-LYP/6-311G+(d,p) level. ^b The experimental values are taken from ref 15.

a quadratic fit to obtain the derivative of the gradient with respect to the reaction coordinate.

Results and Discussions

A. Stationary Points. The optimized geometric parameters of the reactants (CH₃CCl₃ and CH₃CF₃) and products (CH₂CCl₃, CH₂CF₃, and HCl) at the BH&H-LYP/6-311G+(d,p) level of theory are shown in Table 1. The available experimental values¹⁵ are also listed for comparison. The theoretical C–Cl and C–C bond lengths differ from the experimental values just by up to 0.012 Å (*R*_{C–Cl} for CH₃CCl₃) and 0.048 Å (*R*_{C–C} for CH₃CCl₃), respectively. For bond angles, the optimized value of ∠FCC in CH₃CF₃ at BH&H-LYP level, 111.9°, differs from the experimental one, 119.2°,¹⁵ by about 7°. The other theoretical values of ∠FCC in CH₃CF₃ at MP2/6-31+G(d) level by Sheng et al.¹⁶ and HF/6-31G(d) level by Rayez and co-workers⁶ are 112.0° and 111.6°, respectively, and the difference between their theoretical results and experimental values is also about 7° for ∠FCC. The other bond lengths and bond angles obtained at BH&H-LYP/6-311G+(d,p) level are in good agreement with the experimental results.

Geometric parameters of the transition-state structures for both hydrogen-abstraction reactions are listed in Table 2. Both transition states have C_s symmetry, and the angles between the breaking C–H' bond and the nascent H'–Cl bond (∠CH'Cl) are 174.6° for the reaction CH₃CCl₃ + Cl and 177.0° for the reaction CH₃CF₃ + Cl. These results are in good agreement with those obtained by Rayez and co-workers⁶ for the title reactions. The Cl–H' bond lengths of transition states calculated by Rayez and co-workers are slightly larger, and the C–H' bond lengths are somewhat smaller than our corresponding results.

Table 3 gives the harmonic vibrational frequencies (wavenumbers) of the reactants, products, and transition states at the BH&H-LYP/6-311G+(d,p) level, as well as the experimental

TABLE 2: A Comparison of the Calculated Geometrical Parameters (Distance in Å and Angle in deg)^a of the Transition States for the Selected Hydrogen-Abstraction Reactions (X = Cl or F)

geom params	Cl···H···CH ₂ CCl ₃ (C _s) ^b	Cl···H···CH ₂ CF ₃ (C _s) ^b
R _{CC}	1.489	1.490
R _{CX}	1.772	1.326
R _{CH'}	1.412 (1.403)	1.439 (1.411)
R _{H'Cl}	1.443 (1.469)	1.424 (1.460)
R _{CH}	1.079	1.078
R _{CX}	1.796	1.336
∠XCC	110.7	111.9
∠HCC	110.8	114.9
∠H'CC	108.4	106.0
∠CH'Cl	174.6	177.0

^a Obtained at the BH&HLYP/6-311G+(d,p) level. ^b Values in parentheses are from ref 6 obtained at the HF/6-31G(d) level.

TABLE 3: Calculated and Experimental Frequencies (Wavenumbers, cm⁻¹) at Stationary Points for the Two Reactions

species	BH&H-LYP/6-311G+(d,p)	expt
CH ₃ CCl ₃	254, 254, 323, 359, 359,	
	362, 547, 753, 753,	
	1127, 1152, 1152,	
	1478, 1530, 1530,	
	3144, 3230, 3230	
CH ₂ CCl ₃	152, 245, 254, 338, 359,	
	370, 550, 599, 745,	
	745, 1121, 1173,	
	1496, 3251, 3379	
Cl···H···CH ₂ CCl ₃	1268i, 55, 67, 213, 253,	
	305, 358, 364, 462,	
	474, 566, 740, 763,	
	929, 961, 1141, 1156,	
	1219, 1496, 3205, 3312	
CH ₃ CF ₃	238, 377, 377, 562, 562,	–, 365, 365, 541,
	621, 868, 1021, 1021,	602, 830, 970,
	1291, 1291, 1346, 1498,	1233, 1233, 1280,
	1536, 1536, 3152, 3239,	1408, 1443, 1443,
	3239	2975, 3035, 3035 ^a
CH ₂ CF ₃	111, 357, 388, 520, 556,	
	624, 638, 892, 978,	
	1176, 1293, 1354, 1503,	
Cl···H···CH ₂ CF ₃	3261, 3391	
	1204i, 52, 73, 323, 358,	
	419, 491, 558, 567, 634,	
	847, 894, 917, 1016,	
	1149, 1242, 1319, 1355,	
HCl	1504, 3219, 3327	
	3045	2991 ^b

^a Experimental values from ref 18. ^b Experimental values from ref 17.

results.^{17,18} For the species CH₃CF₃ and HCl, the calculated frequencies (wavenumbers) are in excellent agreement with the experimental values, the largest deviation being 7%. The transition states are confirmed by normal-mode analyses, which have only one imaginary frequency and the eigenvector of which corresponds to the direction of the reaction.

The reaction enthalpies and potential barriers calculated at the CCSD(T)//BH&H-LYP level with ZPE correction are listed in Table 4. For CH₃CCl₃ + Cl → CH₂CCl₃ + HCl and CH₃CF₃ + Cl → CH₂CF₃ + HCl reactions, the calculated reaction enthalpies at temperature 298 K are 2.29 and 4.56 kcal/mol, respectively, which are in general agreement with the corresponding experimental values of 0.0 and 4.0 kcal/mol.¹⁹ The reaction potential barriers at the CCSD(T)//BH&H-LYP level are 5.24 kcal/mol for CH₃CCl₃ + Cl → CH₂CCl₃ + HCl reaction and 8.58 kcal/mol for CH₃CF₃ + Cl → CH₂CF₃ + HCl reaction.

TABLE 4: Reaction Enthalpies (ΔH°_{298}) and Forward Potential Barriers (ΔE^\ddagger) (kcal/mol) with ZPE Correction for the Two Reactions

	$\text{CH}_3\text{CCl}_3 + \text{Cl} \rightarrow \text{CH}_2\text{CCl}_3 + \text{HCl}$	$\text{CH}_3\text{CF}_3 + \text{Cl} \rightarrow \text{CH}_2\text{CF}_3 + \text{HCl}$
$\Delta E^\ddagger{}^a$	8.28	10.95
$\Delta E^\ddagger{}^b$	5.24	8.58
$\Delta H^\circ_{298}{}^a$	2.56	5.16
$\Delta H^\circ_{298}{}^b$	2.29	4.56
expt	0.00	4.00

^a Calculations at the BH&H-LYP/6-311+G+(d,p) level. ^b Single-point CCSD(T)/6-311+G(2df,2p) energy calculations at the BH&H-LYP/6-311+G(d,p) geometries. ^c The experimental values from ref 19.

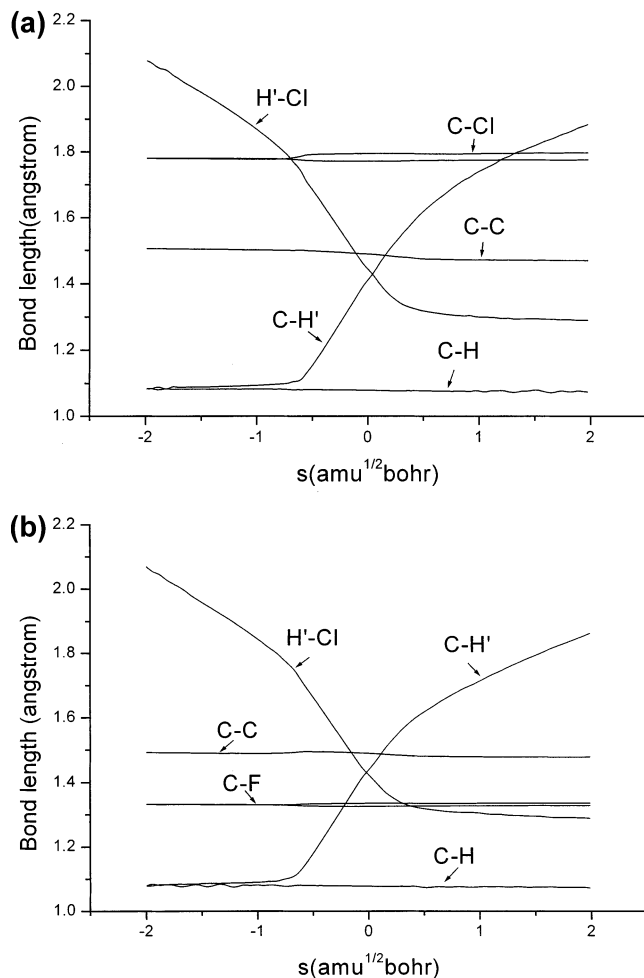


Figure 1. Changes of the bond lengths along the BH&H-LYP/6-311+G(d,p) minimum energy path plotted vs the reaction coordinate s in the mass-weighted coordinates: (a) $\text{CH}_3\text{CCl}_3 + \text{Cl} \rightarrow \text{CH}_2\text{CCl}_3 + \text{HCl}$ reaction; (b) $\text{CH}_3\text{CF}_3 + \text{Cl} \rightarrow \text{CH}_2\text{CF}_3 + \text{HCl}$ reaction.

For both reactions, the calculated ΔE values at the CCSD(T)//BH&H-LYP level are lower than those at the BH&H-LYP level, indicative of the overestimate of the energy barriers for the two H-abstraction processes by the BH&H-LYP method. This highlights the importance of carrying out higher-level single-point energy computations.

B. Minimum Energy Path. The changes of bond length along the IRC for Cl with CH_3CCl_3 and CH_3CF_3 are plotted in Figure 1, parts a and b, respectively. It is easily seen that with the proceeding of both reactions, the active C-H' (breaking) and Cl-H' (forming) bond lengths change very smoothly up to $s = -0.65$ ($\text{amu}^{1/2}$ bohr). After that, both bonds change rapidly up to about $s = 0.30$ ($\text{amu}^{1/2}$ bohr), and later, the changes

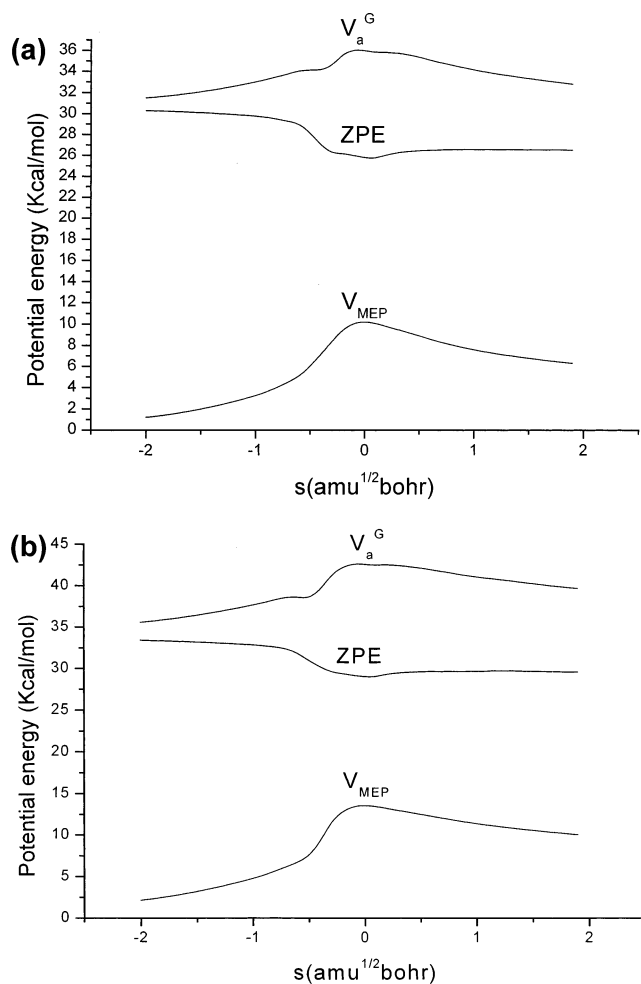


Figure 2. Classical potential energy (V_{MEP}), zero-point energies (ZPE), and vibrational adiabatic potential energy (V_a^G) as a function of the reaction coordinate, s , at the QCISD(T)//BH&H-LYP level: (a) $\text{CH}_3\text{CCl}_3 + \text{Cl} \rightarrow \text{CH}_2\text{CCl}_3 + \text{HCl}$ reaction; (b) $\text{CH}_3\text{CF}_3 + \text{Cl} \rightarrow \text{CH}_2\text{CF}_3 + \text{HCl}$ reaction.

become slow again. However, the remaining bond lengths show almost no change in the entire reaction processes.

The minimum energy path (MEP) based on the intrinsic reaction coordinate theory (IRC) is calculated at the BH&H-LYP level. The potential profile is further refined by the CCSD(T)//BH&H-LYP method. The classical potential energy curves ($V_{\text{MEP}}(s)$) and the ground-state vibrational adiabatic potential energy curves ($V_a^G(s)$) as functions of the intrinsic reaction coordinate s at the CCSD(T)//BH&H-LYP level together with zero-point energy curves ($ZPE(s)$) for two reactions are shown in Figure 2a,b. For both reactions, the maximum positions of V_a^G and V_{MEP} curves are the same, which implies that the variational effect will be small or almost negligible.

C. Rate Constants. The rate constants of the forward reactions are calculated by using conventional transition-state theory (TST) and improved canonical variational transition-state theory (ICVT) with a small-curvature tunneling (SCT) correction for both hydrogen-abstraction reactions over a wide temperature range from 200 to 1200 K at the CCSD(T)//BH&H-LYP level. For the two reactions, the comparison between our theoretical and the experimental rate constants is shown in Table 5, sections a and b, and Figure 3a,b. There are three available experiments^{3,4,6} about the rate constants of the reaction $\text{CH}_3\text{CCl}_3 + \text{Cl} \rightarrow \text{CH}_2\text{CCl}_3 + \text{HCl}$, and these experimental values^{4,6} agree well with each other. Only the values of Wine et al.³ are somewhat larger than the other two. Our calculated rate

TABLE 5: Forward Reaction Rate Constants ($\text{cm}^3 \text{molecule}^{-1} \text{s}^{-1}$) for the Temperature Range 200–1200 K

a. $\text{CH}_3\text{CCl}_3 + \text{Cl} \rightarrow \text{CH}_2\text{CCl}_3 + \text{HCl}$							
<i>T</i> (K)	TST	ICVT	ICVT/SCT ^a	ICVT/SCT ^b	ref 3	ref 4	ref 6
200.0	3.00×10^{-17}	2.36×10^{-17}	1.85×10^{-16}	8.32×10^{-19}			
222.0	1.27×10^{-16}	1.02×10^{-16}	5.46×10^{-16}	4.29×10^{-18}			
259.0	8.50×10^{-16}	7.04×10^{-16}	2.44×10^{-15}	3.93×10^{-17}	2.40×10^{-14}		
298.0	3.96×10^{-15}	3.35×10^{-15}	8.63×10^{-15}	2.41×10^{-16}	3.68×10^{-14}		7.10×10^{-15}
300.0	4.24×10^{-15}	3.59×10^{-15}	9.15×10^{-15}	2.62×10^{-16}			
323.0	8.91×10^{-15}	7.62×10^{-15}	1.71×10^{-14}	6.34×10^{-16}		1.58×10^{-14}	
331.0	1.13×10^{-14}	9.68×10^{-15}	2.09×10^{-14}	8.42×10^{-16}		1.81×10^{-14}	1.23×10^{-14}
356.0	2.23×10^{-14}	1.93×10^{-14}	3.76×10^{-14}	1.90×10^{-15}	7.47×10^{-14}	2.65×10^{-14}	
361.0	2.53×10^{-14}	2.19×10^{-14}	4.20×10^{-14}	2.21×10^{-15}		2.85×10^{-14}	1.97×10^{-14}
390.0	4.98×10^{-14}	4.35×10^{-14}	7.60×10^{-14}	5.00×10^{-15}		4.13×10^{-14}	2.61×10^{-14}
400.0	6.17×10^{-14}	5.40×10^{-14}	9.18×10^{-14}	6.47×10^{-15}		4.63×10^{-14}	
403.0	6.57×10^{-14}	5.75×10^{-14}	9.70×10^{-14}	6.98×10^{-15}		4.79×10^{-14}	
418.0	8.88×10^{-14}	7.80×10^{-14}	1.27×10^{-13}	1.00×10^{-14}		5.62×10^{-14}	4.14×10^{-14}
423.0	9.79×10^{-14}	8.60×10^{-14}	1.38×10^{-13}	1.13×10^{-14}		5.91×10^{-14}	
500.0	3.53×10^{-13}	3.14×10^{-13}	4.41×10^{-13}	5.30×10^{-14}			
600.0	1.24×10^{-12}	1.11×10^{-12}	1.41×10^{-12}	2.42×10^{-13}			
800.0	7.11×10^{-12}	6.41×10^{-12}	7.33×10^{-12}	1.95×10^{-12}			
1000.0	2.33×10^{-11}	2.10×10^{-11}	2.29×10^{-11}	7.92×10^{-12}			
1200.0	5.59×10^{-11}	5.03×10^{-11}	5.34×10^{-11}	2.21×10^{-11}			

b. $\text{CH}_3\text{CF}_3 + \text{Cl} \rightarrow \text{CH}_2\text{CF}_3 + \text{HCl}$					
<i>T</i> (K)	TST	ICVT	ICVT/SCT ^a	ICVT/SCT ^b	ref 7
200.0	9.59×10^{-21}	6.93×10^{-21}	4.27×10^{-20}	5.97×10^{-22}	
240.0	4.30×10^{-19}	3.23×10^{-19}	1.14×10^{-18}	3.42×10^{-20}	
255.0	1.34×10^{-18}	1.01×10^{-18}	3.11×10^{-18}	1.16×10^{-19}	
281.0	7.26×10^{-18}	5.60×10^{-18}	1.41×10^{-17}	7.33×10^{-19}	1.10×10^{-17}
298.0	1.89×10^{-17}	1.47×10^{-17}	3.36×10^{-17}	2.09×10^{-18}	2.49×10^{-17}
300.0	2.10×10^{-17}	1.64×10^{-17}	3.69×10^{-17}	2.34×10^{-18}	2.72×10^{-17}
368.0	4.09×10^{-16}	3.26×10^{-16}	5.62×10^{-16}	6.14×10^{-17}	3.21×10^{-16}
400.0	1.20×10^{-15}	9.66×10^{-16}	1.53×10^{-15}	2.02×10^{-16}	
450.0	4.91×10^{-15}	3.98×10^{-15}	5.74×10^{-15}	9.60×10^{-16}	
500.0	1.56×10^{-14}	1.28×10^{-14}	1.72×10^{-14}	3.46×10^{-15}	
600.0	9.53×10^{-14}	7.83×10^{-14}	9.62×10^{-14}	2.57×10^{-14}	
800.0	1.09×10^{-12}	8.94×10^{-13}	1.00×10^{-12}	3.78×10^{-13}	
1000.0	5.38×10^{-12}	4.42×10^{-12}	4.76×10^{-12}	2.19×10^{-12}	
1200.0	1.70×10^{-11}	1.39×10^{-11}	1.47×10^{-11}	7.71×10^{-12}	

^a Values are calculated at the CCSD(t)/6-311+G(2df,2p)//BH&H-LYP/6-311G+(d,p) level. ^b Values are calculated at the BH&H-LYP/6-311+G(d,p) level.

constants are in good agreement with the experimental ones, that is, the ICVT/SCT rate constants are factors of 1.2, 1.7, and 1.4 higher than the experimental values^{4,6} at 298, 331, and 356 K, respectively, and are 2.1, 2.9, and 3.1 times over the corresponding experimental value⁶ at 361, 390, and 418 K, respectively. However, the temperature dependence of rate constants is somewhat steeper than the measured one. From Figure 3a and Table 5, section a, we can see that our calculated rate constants are somewhat lower than the experimental values,³ but they are in better agreement with the other experimental ones obtained by Tschuikow-Roux et al.⁴ and Rayez and co-workers⁶ Our calculated rate constant at 298 K is also in good agreement with other theoretical result, $6.8 \times 10^{-15} \text{ cm}^3 \text{ molecule}^{-1} \text{ s}^{-1}$, obtained by Rayez and co-workers.

For the reaction $\text{CH}_3\text{CF}_3 + \text{Cl} \rightarrow \text{CH}_2\text{CF}_3 + \text{HCl}$, our calculated rate constants are in good agreement with the experimental ones in the whole temperature range measured and the ICVT/SCT rate constants are factors of 1.3, 1.3, 1.4, and 1.7 higher than the experimental values⁷ at 281, 298, 300, and 368 K, respectively. The theoretical temperature dependence of rate constants agrees well with the experimental one.⁷ Our results within 200–1200 K may present a useful comparison with available experiments. It is worthy of note that for the $\text{CH}_3\text{CF}_3 + \text{Cl}$ reaction, Rayez and co-workers⁶ have obtained the 298 K rate constant as $5.7 \times 10^{-16} \text{ cm}^3 \text{ molecule}^{-1} \text{ s}^{-1}$ with the activation energy of 6.11 kcal/mol at the BAC-MP4/HF/6-31G(d,p) level using ISO-M method. Their value of rate

constant is larger than the experimental value,⁷ $2.49 \times 10^{-17} \text{ cm}^3 \text{ molecule}^{-1} \text{ s}^{-1}$, and the activation energy is smaller than the experimental value, 7.90 kcal/mol. Our 298 K results ($3.36 \times 10^{-17} \text{ cm}^3 \text{ molecule}^{-1} \text{ s}^{-1}$ and 8.70 kcal/mol) are much closer to the experimental values.⁷ In addition, Rayez and co-workers did not report the rate constants at other temperatures besides 298 K.

From Table 5, section a and b, we can see that the ICVT/TST ratios are less than 1.4, and this indicates that the variational effects are small on the rate constants for the two reactions. For the SCT effect, at 200, 300, and 400 K, the ICVT/SCT rate constants at CCSD(T)/6-311+G(2df,2p)//BH&H-LYP/6-311+G(d,p) level are about 7.8, 2.5, and 1.7 times over the ICVT values for the reaction $\text{CH}_3\text{CCl}_3 + \text{Cl}$ and 6.2, 2.3, and 1.6 times over the ICVT values for the reaction $\text{CH}_3\text{CF}_3 + \text{Cl}$, respectively, whereas between 800 and 1200 K, the differences between ICVT and ICVT/SCT rate constants become very small, which indicates that the small-curvature tunneling effect is only important in the lower temperature range.

Conclusions

In this paper, the hydrogen-abstraction reactions from 1,1,1-trichloroethane and 1,1,1-trifluoroethane by chlorine atoms are investigated theoretically. The respective forward potential barriers for both reactions, calculated at the CCSD(T)//BH&H-LYP level, are 5.24 and 8.58 kcal/mol, and the respective

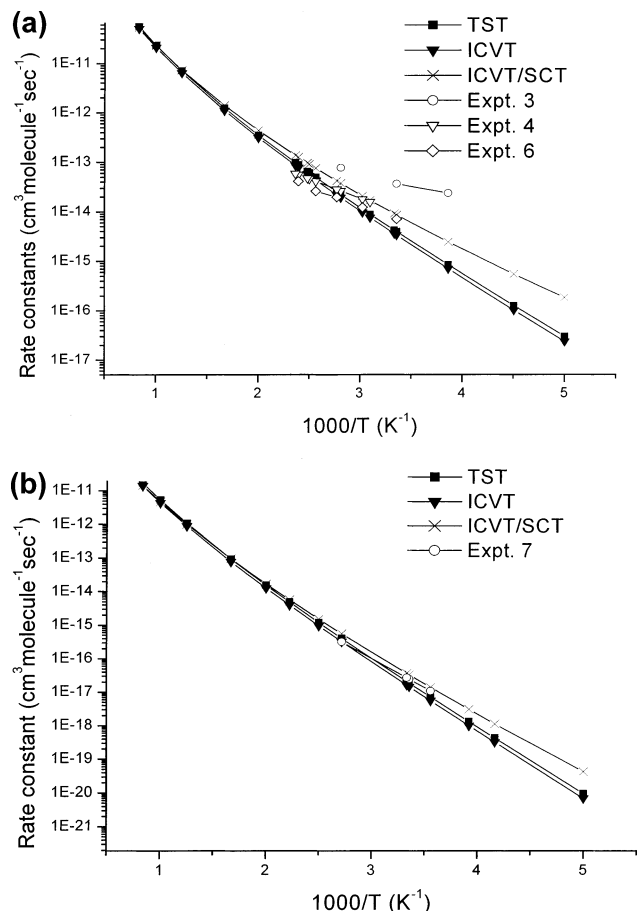


Figure 3. Computed TST, ICVT, and ICVT/SCT rate constants as a function of $10^3/T$ and available experimental values: (a) $\text{CH}_3\text{CCl}_3 + \text{Cl} \rightarrow \text{CH}_2\text{CCl}_3 + \text{HCl}$ reaction; (b) $\text{CH}_3\text{CF}_3 + \text{Cl} \rightarrow \text{CH}_2\text{CF}_3 + \text{HCl}$ reaction.

reaction enthalpies are 2.29 and 4.56 kcal/mol. Both transition states have C_s symmetry. The rate constants in the temperature range 200–1200 K are calculated by the conventional transition-state theory (TST) and improved canonical variational transition-state theory (ICVT) with a small-curvature tunneling (SCT) correction. For both reactions, the calculated rate constants are in good agreement with the experimental values over the measured temperature range. The variational effect is small, and the small-curvature tunneling effect is only important in the lower temperature range on the rate constants for both reactions.

Acknowledgment. The authors thank Professor Donald G. Truhlar for providing the POLYRATE 8.4.1 program. This work is supported by the National Science Foundation of China (Grants 29892168, 20073014), Doctor Foundation by the

Ministry of Education, Foundation for University Key Teacher by the Ministry of Education, and Key subject of Science and Technology by the Ministry of Education of China.

References and Notes

- (1) Thomas, P. J. *Current Topic in Mass Spectrometry and Chemical Kinetics*; Heydon and Sons: London, 1982; p 115.
- (2) Cillien, C.; Goldfinger, P.; Huybrechts, G.; Martens, G. *Trans. Faraday. Soc.* **1967**, *63*, 1631.
- (3) Wine, P. H.; Semmes, D. H.; Ravishankara, A. R. *Chem. Phys. Lett.* **1982**, *90*, 128.
- (4) Tschuikow-Roux, E.; Niedzielski, J.; Faraji, F. *Can. J. Chem.* **1985**, *63*, 1093.
- (5) Atkinson, R.; Baulch, D. L.; Cox, R. A.; Hampson, R. F.; Keer, J. A.; Troe, J. *J. Phys. Chem. Ref. Data* **1992**, *21*, 1437.
- (6) Talhaoui, A.; Louis, F.; Devolder, P.; Meriaux, B.; Sawerysyn, J.-P.; Rayez, M.-T.; Rayez, J.-C. *J. Phys. Chem.* **1996**, *100*, 13531.
- (7) Tschuikow-Roux, E.; Yano, T.; Niedzielski, J. *J. Chem. Phys.* **1985**, *82*, 65.
- (8) Histsuda, K.; Takahashi, K.; Matsumi, Y.; Wallington, T. J. *J. Phys. Chem. A* **2001**, *105*, 5131.
- (9) Senkan, S. M.; Quam, D. *J. Phys. Chem.* **1992**, *96*, 10837.
- (10) Frisch, M. J.; Trucks, G. W.; Schlegel, H. B.; Scuseria, G. E.; Robb, M. A.; Cheeseman, J. R.; Zakrzewski, V. G.; Montgomery, J. A., Jr.; Stratmann, R. E.; Burant, J. C.; Dapprich, S.; Millam, J. M.; Daniels, A. D.; Kudin, K. N.; Strain, M. C.; Farkas, O.; Tomasi, J.; Barone, V.; Cossi, M.; Cammi, R.; Mennucci, B.; Pomelli, C.; Adamo, C.; Clifford, S.; Ochterski, J.; Petersson, G. A.; Ayala, P. Y.; Cui, Q.; Morokuma, K.; Malick, D. K.; Rabuck, A. D.; Raghavachari, K.; Foresman, J. B.; Cioslowski, J.; Ortiz, J. V.; Boboul, A. G.; Stefanov, B. B.; Liu, G.; Liashenko, A.; Piskorz, P.; Komaromi, I.; Gomperts, R.; Martin, R. L.; Fox, D. J.; Keith, T.; Al-Laham, M. A.; Peng, C. Y.; Nanayakkara, A.; Gonzalez, C.; Challacombe, M.; Gill, P. M. W.; Johnson, B. G.; Chen, W.; Wong, M. W.; Andres, J. L.; Gonzalez, C.; Head-Gordon, M.; Replogle, E. S.; Pople, J. A. *Gaussian 98W*, revision A.7; Gaussian, Inc.: Pittsburgh, PA, 1998.
- (11) Chang, Y.-Y.; Corchado, J. C.; Fast, P. L.; Villa, J.; Hu, W.-P.; Liu, Y.-P.; Lynch, G. C.; Jackels, C. F.; Nguyen, K. A.; Gu, M. Z.; Rossi, I.; Coitino, E. L.; Clayton, S.; Melissas, V. S.; Lynch, B. J.; Steckler, R.; Garrett, B. C.; Isaacson, A. D.; Truhlar, D. G. *POLYRATE*, version 8.4.1; University of Minnesota: Minneapolis, MN, 2000.
- (12) Garrett, B. C.; Truhlar, D. G.; Grev, R. S.; Magnuson, A. W. *J. Phys. Chem.* **1980**, *84*, 1730.
- (13) Truhlar, D. G.; Isaacson, A. D.; Garrett, B. C. Generalized Transition State Theory. In *The Theory of Chemical Reaction Dynamics*; Baer, M., Ed.; CRC Press: Boca Raton, FL, 1985; Vol. 4, p 65.
- (14) Steckler, R.; Hu, W.-P.; Liu, Y.-P.; Lynch, G. C.; Garrett, B. C.; Isaacson, A. D.; Melissas, V. S.; Lu, D.-P.; Troung, T. N.; Rai, S. N.; Hancock, G. C.; Lauderdale, J. G.; Joseph, T.; Truhlar, D. G. *Comput. Phys. Commun.* **1995**, *88*, 341.
- (15) Lide, D. R., Ed. *CRC Handbook of Chemistry and Physics*, 80th ed.; CRC Press: Boca Raton, FL, 1999–2000.
- (16) Sheng, L.; Li, Z. S.; Xiao, J. F.; Liu, J. Y.; Sun, C. C. *Chem. Phys.* **2002**, *282*, 1.
- (17) *JANAF Thermochemical Tables*, 2nd ed.; National Standard Reference Data Series; National Bureau of Standards: Washington, DC, 1986; Vol. 37.
- (18) Lafon, B.; Rud Nielsen, J. *J. Mol. Spectrosc.* **1966**, *21*, 175.
- (19) DeMore, W. B.; Sander, S. P.; Golden, D. M.; Hampson, R. F.; Kurylo, J.; Howard, C. J.; Ravishankara, A. R.; Kolb, C. E.; Molina, M. J. *Chemical Kinetics and Photochemical Data for Use in Stratospheric Modeling*; Evaluation No. 11, Publication 94-26, Jet propulsion Laboratory: Pasadena, CA, 1994.